Am J Transl Res 2021;13(5):4266-4280
www.ajtr.org /ISSN:1943-8141/AJTR0128173

Original Article

PRICKLE1 promotes gastric cancer metastasis by activating mTOR signaling

Rongjian Zhou[1,2*], Zhaoqing Tang[1,2*], Haojie Li[1,2], Xuefei Wang[1,2], Yihong Sun[1,2]

[1]Department of General Surgery, Zhongshan Hospital, Fudan University, Shanghai 200032, China; [2]Gastric Cancer Center, Zhongshan Hospital, Fudan University, Shanghai 200032, China. [*]Equal contributors.

Received December 13, 2020; Accepted March 2, 2021; Epub May 15, 2021; Published May 30, 2021

Abstract: Lymph node metastasis confers an unfavorable prognosis in gastric cancer (GC). Transcriptomic sequencing has been used to explore the molecular changes in metastatic cancers, but the changes of expression profiling of metastatic GC in lymph nodes remain largely unknown. To identify the potential driver genes, we performed whole transcriptomic sequencing (RNA-seq) on five pairs of gastric adenocarcinoma specimens with metastatic lymph nodes confirmed by pathology. We identified six genes associated with lymph node metastasis and predicted poor prognosis in GC patients. Finally, we focused on PRICKLE1, a cell polarity protein, which dramatically upregulated in several GC cell lines from metastatic lesions compared with those from the primary tumor. Loss and gain of function assay in vitro showed that the migration and invasion capability of GC cells were limited by downregulating and upregulating PRICKLE1 expression. Mechanically, we found PRICKLE1 might modulate tumor metastasis through mTOR signaling pathway. Inhibition of mTOR significantly reduced GC cell migration and invasion in vitro. In summary, we identified and validated PRICKLE1 as a novel gene involved in GC metastasis. This study provided a valuable insight into the mechanisms of GC metastasis and developed a potential therapeutic target to prevent GC cell dissemination.

Keywords: Gastric cancer, lymph node metastasis, transcriptomic sequencing, PRICKLE1

Introduction

Gastric cancer (GC) is one of the most prevalent malignant tumors and the leading cause of cancer mortality around the world, spatially in the east of Asia [1, 2]. In China, an estimated 680000 new cases of GC are diagnosed and about 490000 patients are reported to death from GC each year [1]. Most patients have been involved in advanced stages with metastatic conditions before operation, which reduced the survival benefit of post-operational treatments [3]. Several researches have indicated that the majority of epithelial cancers from gastrointestinal organs, including GC, preferentially developed metastatic lesions by spreading via lymphatic vessels [4]. Lymph node metastasis (LNM) is more common than hepatic metastasis and peritoneal seeding during GC progression. During the early stage, up to 10% intramucosal GC and 20-30% submucosal GC developed LNM [5, 6]. However, this number raised to 60% in advanced GC. Although the effect of LNM on reduced survival in GC, the underlying driver genes and mechanisms remain unclear.

Lymphatic metastasis has received much attention in recent years due to its strong indication of distant metastasis and local recurrence during cancer progression [7, 8]. Indeed, lymphatic metastasis comprises a series of events, including cancer cell proliferation, migration, invasion, the resistance of anoikic, and the formation of new lymphatic vessels in the tumor microenvironment. Surprising evidence indicated that lymphatic vessels even promote malignant tumor cell recruitment from the primary site to lymph nodes (LNs) [9, 10]. Recently, research suggested that cancer cells from metastatic LNs showed more resistance to ferroptosis and formed more metastasis, which indicated that exposure to the lymphatic microenvironment can further protect cancer cells from ferroptosis and increase the capability to survive during metastasis through the blood [11]. Another study focused on the integrated omics

features of metastatic colorectal cancer and revealed that the proteomic profiling of metastatic tumors showed obvious differences from that of primary tumors [12]. These researches suggested that metastatic tumors may exhibit a more aggressive phenotype in the lymphatic microenvironment compared with primary tumors, which may account for distant metastasis and therapeutic resistance [13]. Moreover, it has been demonstrated that metastatic tumors presented a greater monoclonal proportion compared with primary tumors, which indicated that metastatic tumors were derived from the same ancestral clones [12]. These metastatic clones can trigger tumor cells to further spreading to distant organs [14]. Therefore, focusing on the biological feature of metastatic tumors is essential for understanding the mechanism of tumor metastasis and discovering novel therapeutic targets.

In this study, we aimed to identify driver genes that preferentially altered within metastatic GC cells from lymph nodes compared with the primary tumors and elucidate potential mechanisms. Transcriptomic sequencing was performed on pathologically confirmed metastatic lymph nodes (tumor proportion ≥ 80%) and paired primary tumors. We identified several crucially upregulated genes in metastatic lymph nodes and focused on prickle planar cell polarity protein 1 (PRICKLE1), which have been reported to serve as a considerable regulator of breast cancer metastasis, but its function in GC remains unknown. By functional assay, we found that PRICKLE1 contributed to migration and invasion of GC cells by activating the mTOR pathway. In summary, we identified PRICKLE1 as a novel gene for GC metastasis, which may provide a new therapeutic target to inhibit GC cell dissemination.

Materials and methods

Patients and specimens

GC patients with a diameter ≥ 1 cm metastatic lymph node measured by pre-operational computed tomography were enrolled in this study. The metastatic status and proportion in the involved lymph node were confirmed by HE stains and the metastatic percentage ≥ 80% was adopted for further analysis. The collection and use of human tissues were approved by the Ethical Committee of Zhongshan Hospital of Fudan University (Approved No: B2020-263). Written informed consent was obtained by all the patients. The study protocol followed the ethical guidelines of the Declaration of Helsinki.

RNA-seq and data analysis

Total RNA was extracted by Trizol reagent according to the manufacture's protocol (Invitrogen, Carlsbad, CA, USA). The purity and integrity of the extracted RNA were confirmed using an Agilent Bioanalyzer. Libraries prepared from 100 ng total RNA were further applied for sequencing based on an Illumina Hiseq 2500. Row reads were mapped to mm9 using the TopHat version 1.4.1 program. The Cufflinks version 1.3.0 software was used to assigned fragment per kilobase per million (FPKM) as the expression of each gene. We further applied Cuffdiff software to identify differentially expressed genes between primary tumor and metastatic tumor in lymph nodes. Genes with a $\log_2$(FoldChange) and -$\log_{10}$(*P* value)>|1.5| were identified as the differentially expressed genes. Differentially expressed genes heat map was clustered by k-means clustering using the Euclidean distance as the distance.

GC gene expression from ACRG cohort and data analysis

Gene expression data and clinical information of GC from the Asian cancer research group (ACRG) cohort (GSE62254) and GSE26253 were derived from GEO (https://www.ncbi.nlm.nih.gov/geo/). Genes highly expressed in patients with metastatic nodes were selected by GEO2R (https://www.ncbi.nlm.nih.gov/geo/geo-2r/). The highly expressed overlap genes between GCs with metastatic nodes from the ACRG cohort and clinical samples from this study were further selected for evaluating the prognostic significance by Kaplan-Meir plotter tool (https://kmplot.com/analysis/). The expression profile of the ACRG cohort was divided into different groups according to the medium value of PRICKLE1 and gene set enrichment analysis (GSEA) was conducted by GSEA software version 4.1.0 (Broad Institute, CA, USA) to dissect the signaling pathways significantly associated with PRICKLE1 level (PRICKLE1^{high} vs PRICKLE1^{low}). The Cancer Cell Line Encyclopedia (CCLE) project was launched and maintained by the Broad Institute, the Novartis Institutes for Biomedical Research, and its Ge-

nomics Institute of the Novartis Research Foundation, which contained most of the GC cell lines. We downloaded the RNA-seq data of 15 common GC cell lines for further analysis.

Quantitative real-time PCR (qRT-PCR)

Total RNA from clinical samples and cells was isolated using Trizol reagent according to the manufacture's protocol (Invitrogen, Carlsbad, CA, USA). Complementary DNA (cDNA) was synthesized from total RNA using PrimerScrip RT reagent Kit (Takara, Dalian, China). RT-PCR was performed using SYBR Green PCR master mix (Takara, Dalian, China). 18S-RNA served as an internal control. PCR was run on the QuantStudio™ 7 Flex Real-Time PCR System (Applied Biosystems, Foster City, CA, USA) and data were analyzed by the $2^{-\Delta\Delta CT}$ method. The primers were listed in the Supplementary Table 1.

Cell culture and reagents

Human gastric cancer cell lines HGC27 and MGC803 were purchased from the Institute of Biochemistry and Cell Biology of the Chinese Academy of Science, Shanghai, China. The cell was cultured in Dulbecco's modified Eagle's medium (DMEM) (Hyclone, UT, USA) supplemented with 10% fetal bovine serum (FBS), 100 U/ml penicillin, and 100 mg/ml streptomycin (Invitrogen, Carlsbad, CA, USA) in humidified air at 37°C with 5% CO_2.

siRNA transfection

HGC27 cell was transfected with the indicated siRNA (10 μM) using RNAiMax transfection reagent (Invitrogen, Carlsbad, CA, USA) according to the manufacturer's instructions. The following sequences of siRNA referring to Daulat et al. [15] were used to target PRICKLE1 (#1) GAGAGAAGCAUCGGAUUAATT, PRICKLE1 (#2) GAAGAUAAAUGGAGGUGAATT. The protein and RNA extraction were collected for detecting the knockdown efficiency by Western blot and real-time PCR after 48 hours of transfection.

Cell migration and invasion assay

Cell migration capabilities were detected by Transwell chambers (Corning, NY, USA) assay as previously described. The Transwell chambers precoated with Matrigel matrix (BD science, MD, USA) were applied to analyze the cell invasion capabilities. After 24 hours of transfection with siRNA, cells were seeded into up chambers (5×10^5/chambers) without FBS and the number of cells that migrated or invaded the down surface of the chamber was calculated by microscope after 24 hours. All experiments were repeated in triplicate.

Wound healing assay

About 1×10^6 cells were seeded into six-well plates at 37°C with 5% CO_2 overnight. Then the cell was gently scraped with a 20 ul pipette tip. The cells were washed by phosphate-buffered saline and cultured in DMEM without FBS. After scratching, cells were photographed by a microscope every 24 hours in the scratched site. The percentage of the wound closure represented the capability of migration.

Actin assay

The procedure of actin assay was described in previous research by Qiao [16]. Indicated cells were seeded in 10 cm dish and lysed directly by actin stabilization buffer (50 mM PIPES [pH 6.9], 50 mM NaCl, 5 mM $MgCl_2$, 5 mM EGTA, 2 mM ATP, 5% glycerol, 0.1% NP-40, 0.1% Triton X-100, 0.1% Tween 20, 0.1% β-mercaptoethanol, 1:100 protease inhibitor and 1:100 phosphatase inhibitor) for 10 min at 37°C. Then cells were scraped into Eppendorf tubes and centrifuged at 300×g at 37°C. The protein was adjusted to equal concentration by the Bradford method. 10% of the cell lysates were separated as "total input". The G-actin and F-actin were separated at 100,000×g for 1 hour at 37°C. After centrifugation, G-actin remains in the supernatant while F-actin sediments. The supernatant was removed to a new Eppendorf tube while the sediment was dissolved in 1 μM cytochalasin D (Sigma-Aldrich) and kept in ice for 45 min. Finally, all samples were added 1% SDS loading buffer and boiled, followed by western blotting.

Western blot

The cells and tissues were lysed by RIPA solution (Beyotime, Shanghai, China) complemented with protease inhibitor cocktail and phosphatase inhibitor cocktail (Sigma, USA). All samples were diluted to achieve the same concentration using the Bradford method accord-

ing to the manufacturer's instruction. Then proteins were added to 10% SDS-PAGE gel with 20 μg per well, followed by transfer to polyvinylidene difluoride (PVDF) membrane. The membrane was blocked in 5% skim milk and incubated with the following primary antibodies at 4°C overnight: PRICKLE1 (1:1000, Santa Cruz Biotechnology, sc-393034), Phospho-mTOR (Ser2448) (1:1000, Cell signaling Technology, #5536), mTOR (1:1000, Cell signaling Technology, #2972), Phospho-S6RP (Ser235/236) (1:1000, Cell signaling Technology, #4858), β-actin (1:1000, Abcam, ab32572), GAPDH (1:1000, Santa Cruz Biotechnology, sc-20356).

Immunohistochemistry and immunofluorescence

Immunohistochemical staining was performed to detect the PRICKLE1 expression in GC tissues and metastatic lymph nodes. Briefly, tissue sections were deparaffinized in xylene and dehydrated in graded ethanol. Then, 3% hydrogen peroxide was used to block endogenous peroxidase. Primary antibody of PRICKLE1 (1:500, Santa Cruz Biotechnology, sc-393034) was applied to detect protein expression. The staining intensity was categorized as follows: 0, negative; 1, weak; 2, moderate; 3, strong. The staining extent was categorized as follows: 0, <5%; 1, 5-25%; 2, 26-50%; 3, 51-75%; 4, 76-100%. The staining score was computed by multiplying staining intensity and extent. The cytoskeleton was detected by Immunofluorescence of phalloidin staining. Detailly, HGC27 cells transfected with siRNA targeting PRICKLE1 were plated in twelve-well plates (1×10^5/well) containing glass coverslips overnight. Then, the cells were fixed with 4% paraformaldehyde for 15 minutes at room temperature. After blocking with 10% goat serum, the cells were incubated with Alexa Fluor 488 Phalloidin dye (1:1000, Cell signaling Technology, #8878) with 3% bull serum albumin for 1 hour at room temperature. Subsequently, the cells were incubated with DAPI for five minutes. The glass coverslips were visualized under a fluorescence microscope (Carl Zeiss, Jena, Germany).

Statistical analysis

The data were analyzed in the SPSS version23 (IBM, Armonk, USA). Data were presented as the mean ± SEM. A two-tailed Student *t*-test was used to determine significant differences between groups. Pearson's Chi-square test was used to assess the differences of categorical data. Differences were considered statistically significant when $P<0.05$.

Results

Identification of aberrantly upregulated genes in metastatic GC from LNs

We conducted RNA-seq from clinical samples to screen out upregulated genes in metastatic GC from LNs. The workflow was shown in **Figure 1**. By analyzing the data, we identified 978 protein-coding genes upregulated ($\log_2$FoldChange ≥ 1.5 and $-\log_{10}P$-value ≥ 1.5) in metastatic LNs (**Figure 2A**). The heat map displayed the top 50 upregulated and 50 downregulated genes (**Figure 2B**). The detailed information of the top 50 upregulated genes was listed in Supplementary Table 2. To further investigate the crucial genes involved in GC migration and metastasis, differently expressed genes in GC patients with positive nodes compared with those with negative nodes from the ACRG cohort were generated by the GEO2R tool and 1359 protein-coding genes were identified. The overlap analysis showed 18 genes were consistently upregulated (**Figure 2C**). Then we focused on six of the 18 genes that were previously reported in tumorigenesis and metastasis, including PIK3IP1, PRICKLE1, NTRK3, FBLN1, PTGER3, and PGM5. The description and expression of the six genes were listed in **Table 1**. To validate the expression of selected genes, we investigated the expression in the primary tumor and metastatic LNs by RT-qPCR and found the indicated genes highly expressed in metastatic LNs among almost all patients (**Figure 2D**). Consequently, we screened out six oncogenes potentially involved in GC progression and metastasis.

Upregulation of the six genes was correlated with LNM and unfavorable prognosis in GC

To further explore the association between the six gene expression and clinical characteristics, the indicated gene expression profile and clinical information of the ACRG cohort were analyzed. The metastatic lymph node ratio was calculated by comparing the number of positive nodes to all retrieved lymph nodes. We showed that higher expression of the six genes was associated with a higher metastatic lymph no-

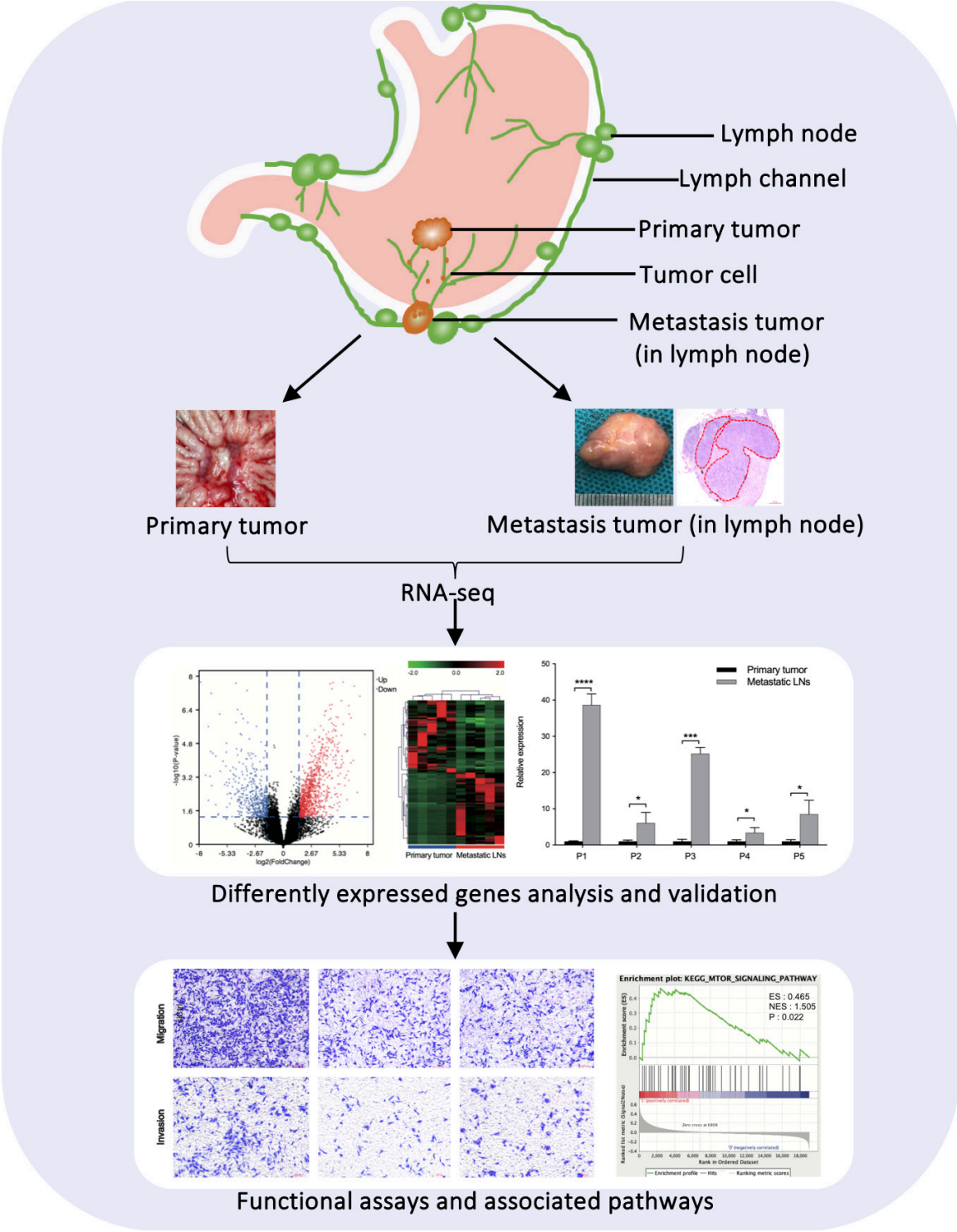

Figure 1. The detailed model pattern of this study was described.

de ratio, which indicated that these selected genes may predict a higher lymphatic metastasis risk in GC (**Figure 3A**). Peritoneal seeding is common among late-stage GC patients and predicts shorter survival. The extent of lymphatic metastasis is a crucial risk factor of peritoneal seeding, which indicates more cancer cells disseminate from the primary tumor. We then found high expression of the six genes was positively correlated with peritoneal seed-

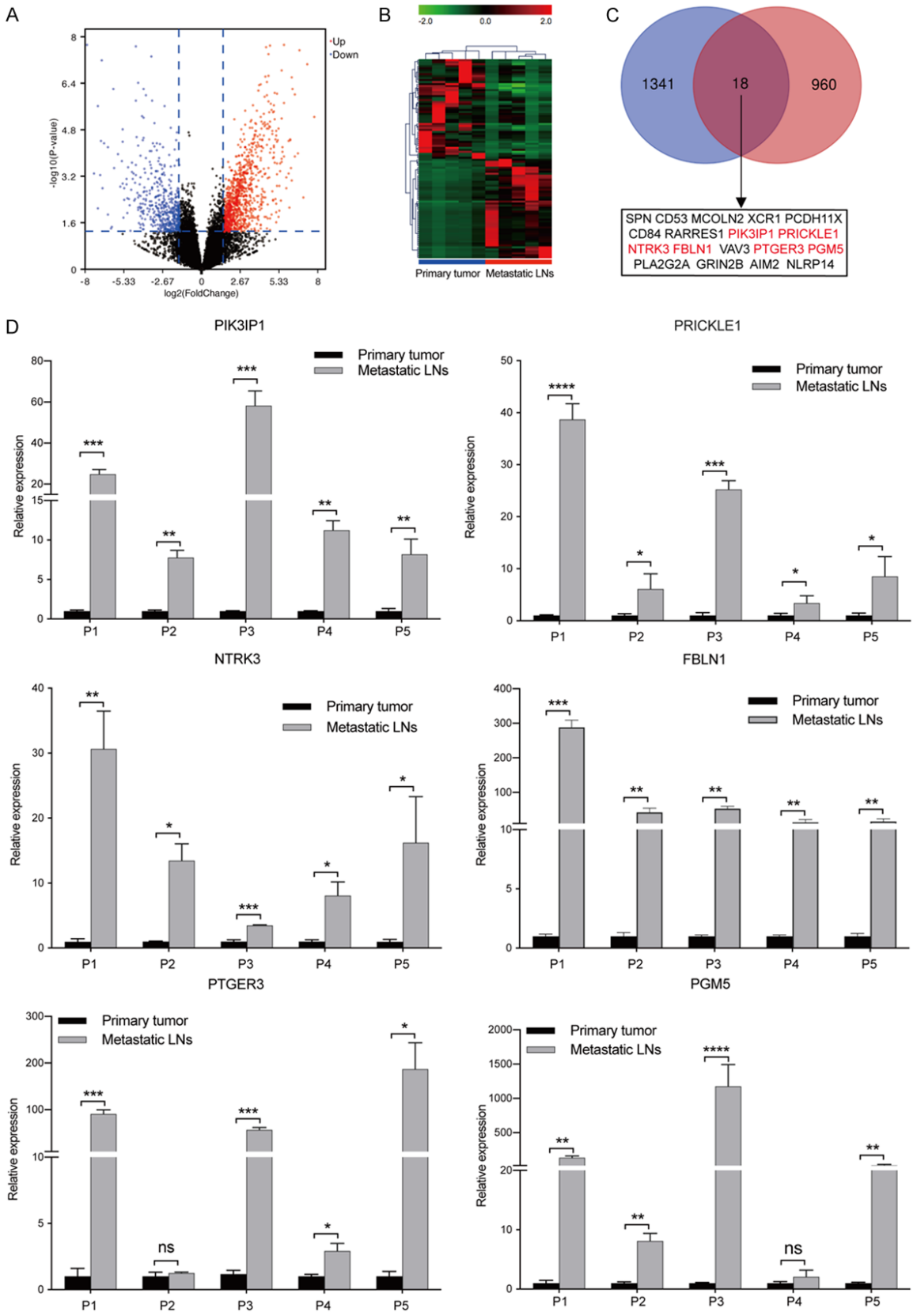

Figure 2. Identification and validation of aberrantly upregulated genes in metastatic GC from lymph nodes by RNA-seq. A: The volcano plot of differently expressed genes (DEGs) of metastatic GC from lymph nodes compared with

primary GC. Genes with a $\log_2$(FoldChange) and -$\log_{10}$(*P* value)>|1.5| were identified as DEGs. B: The heat map of top 50 upregulated and downregulated genes in metastatic GC from lymph nodes. C: The Venn diagram of overlap upregulated genes between metastatic GC from lymph nodes and GC with positive lymph nodes in the ACRG cohort. The mRNA expression of the genes with red color was validated subsequently. D: The expression of six genes associated with cancer progression and metastasis was validated by qRT-PCR. 18s-RNA was considered as an internal control. **P*<0.05, ***P*<0.01, ****P*<0.001, P1, Patient#1.

ing status (Supplementary Figure 1). Kaplan-Meier survival analysis showed a poorer overall survival of GC patients with high expression of the six genes (**Figure 3B**). These results indicated that upregulation of these six genes may participate in the metastasis process during GC progression.

PRICKLE1 was upregulated in metastatic GC and associated with shorter recurrence-free survival

PRICKLE1, prickle planar cell polarity protein 1, belongs to the planar cell polarity pathway and plays a physiological role in epithelial tissue morphogenesis during the embryonic development of invertebrates and vertebrates. The planar cell polarity pathway was described to play a prominent role in cancer cell dissemination and metastasis. Several researches suggested that PRICKLE1 promotes breast cancer cell migration by regulating focal adhesion and actin cytoskeleton reorganization. However, the function of PRICKLE1 in gastric cancer remains unknown. We explored the association between PRICKLE1 expression and clinical pathological characteristics in the ACRG cohort and found high PRICKLE1 expression correlated with Venous invasion and TNM stages (Supplementary Table 3). To explore the relationship between PRICKLE1 expression and metastatic capability, we downloaded RNA-seq data of 15 common GC cell lines from the CCLE project. We then assigned the above cell lines into three groups according to the origin sites, including six cell lines from the primary tumor (containing SUN-719, SNU-1, ECC10, SNU620, IM95, AGS), six cell lines from metastatic lymph nodes (containing MKN7, NUGC-4, MKN1, HGC27, SNU-216, NUGC2,) and three cell lines from hepatic metastasis (containing MKN45, NCI-N87, MKN74). We found a higher PRICKLE1 expression level in metastatic GC cell lines compared with primary ones (**Figure 4A**, **4B**). To validate the PRICKLE1 expression in different cell lines, we explored the endogenous level of PRICKLE1 by qRT-PCR and found a significantly high expression in metastatic cell lines compared with AGS, which originated from a primary tumor (**Figure 4C**). We also showed consistent results of protein level by Western blot (**Figure 4D**). To confirm PRICKLE1 expression in metastatic lymph nodes, immunohistochemistry was performed in six GC patients with positive lymph nodes. Results showed that PRICKLE1 dramatically upregulated in metastatic lymph nodes compared with primary GC (**Figure 4E**). We further validated the result by Weston blot (**Figure 4F**). Survival analysis showed that high expression of PRICKLE1 was associated with shorter recurrence-free survival in GSE26253 (**Figure 4G**). These results indicated that PRICKLE1 overexpressed in GC cells with a higher metastatic capability and contributed to early recurrence in GC.

PRICKLE1 promoted GC cell migration and invasion in vitro

To investigate the biological functions of PRICKLE1 in GC, siRNAs were designed and transfected into HGC27, while overexpressing PRICKLE1 plasmid was constructed in pcDNA3.1 and transfected into MGC803. The knockdown and overexpression efficiency of siRNA targeting PRICKLE1 was validated by western blot. Wound healing assay showed that downregulation of PRICKLE1 significantly inhibited GC cell migration capability, while overexpression of PRICKLE1 promoted GC cell migration capability (**Figure 5A**). Transwell assay also showed downregulation of PRICKLE1 notably suppressed the ability of migration and invasion (**Figure 5B**). When we overexpressed PRICKLE1, the migration and invasion capability of GC cells was promoted (**Figure 5C**). As the major component of the cytoskeleton, actin polymerization plays a critical role in cell migration. Immunofluorescence of phalloidin staining in HGC27 displayed low actin aggregation when PRICKLE1 was inhibited (**Figure 5D**). By ultracentrifugation, we also showed polymerized actin (F-actin) was reduced at low PRICKLE1 cells (**Figure 5E**). These results indicated that PRICKLE1 acted as a fundamental role in GC cell migration and metastasis.

Table 1. Expression and description of genes associated with lymphatic metastasis and poor prognosis in GC

Gene symbol	Gene Full Name	Log_2FoldChage	*P* vale	Functions
PIK3IP1	phosphoinositide-3-kinase interacting protein 1	2.634	<0.0001	A regulator of PI3K/AKT/mTOR pathway
PRICKLE1	prickle planar cell polarity protein 1	2.168	0.001	A regulator of the Wnt/beta-catenin pathway and play a prominent role in cancer cell dissemination
NTRK3	neurotrophic receptor tyrosine kinase 3	5.075	<0.0001	Phosphorylate the members of the MAPK pathway
FBLN1	Fibulin 1	2.756	0.005	A secreted glycoprotein that becomes incorporated into a fibrillar extracellular matrix
PTGER3	prostaglandin E receptor 3	1.937	0.040	One of four receptors identified for prostaglandin E2 (PGE2)
PGM5	phosphoglucomutase 5	1.536	0.048	Phosphotransferase involved in interconversion of glucose-1-phosphate and glucose-6-phosphate

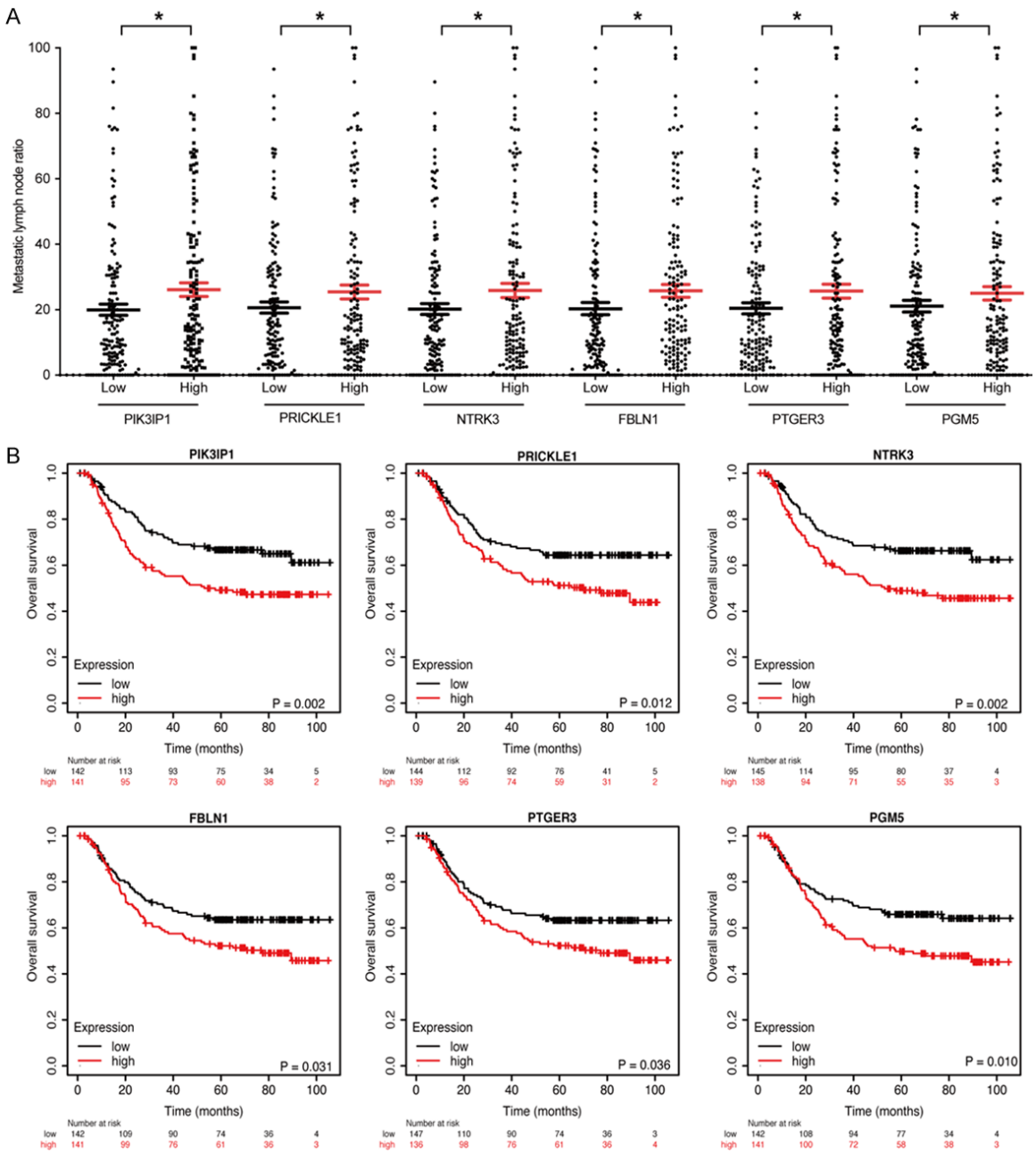

Figure 3. The association between metastasis conditions and the expression of the indicated six genes and their prognostic significance in the ACRG cohort. A: The relationship between metastatic lymph node ratio and the expression of the six upregulated genes in metastatic GC. B: The Kaplan-Meier analysis of the six genes in the ACRG cohort. All patients were divided into low and high groups according to the median value of indicated gene. *P<0.05, **P<0.01, ***P<0.001. ACRG, Asian cancer research group.

PRICKLE1 promoted metastasis by activating mTOR pathway

To investigate the signaling pathways modulated by PRICKLE1, we conducted Gene Sets Enrichment Analysis (GSEA) based on ACRG expression data. All patients were divided into two groups according to the medium value of PRICKLE1 expression and significantly regulated signaling pathways were identified by GSEA software (version 4.1.0). We found mTOR signaling pathway was enriched in GC with a high PRICKLE1 level (**Figure 6A**), which indicated PRICKLE1 may regulate GC migration and

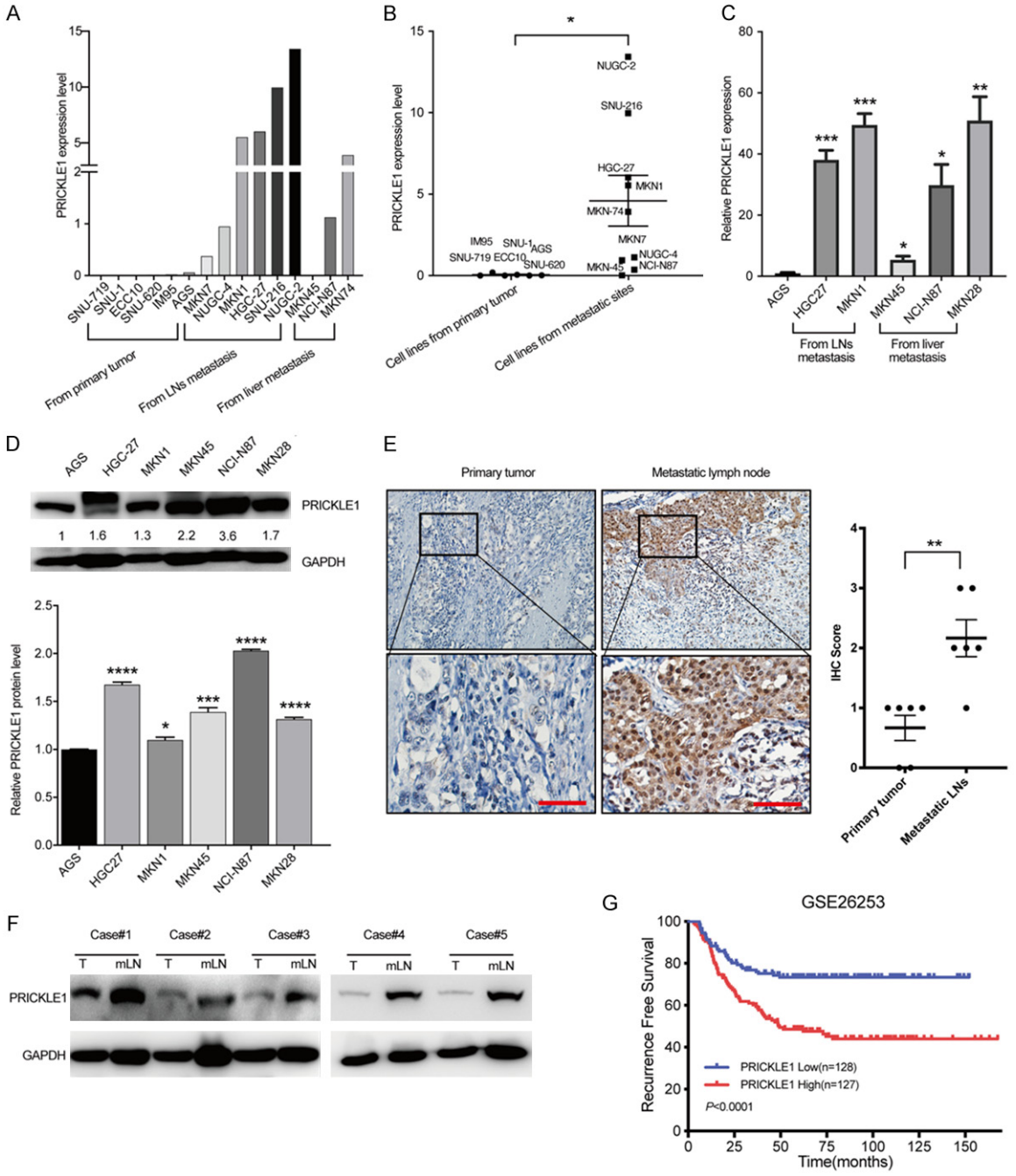

Figure 4. PRICKLE1 was upregulated in metastatic GC and associated with shorter recurrence-free survival. A, B: The PRICKLE1 expression in GC cell lines from CCLE project. C: The mRNA expression of PRICKLE1 was validated in GC cell lines by qRT-PCR. D: The protein expression of PRICKLE1 in GC cell lines was validated by western blot. E: Immunohistochemical staining of PRICKLE1 in primary GC and paired metastatic GC from six patients with positive lymph nodes confirmed by pathology. Scale bar: 100μm. F: The protein expression of PRICKLE1 in primary and metastatic GC from lymph nodes was analyzed by western blot. G: The recurrence-free survival of PRICKLE1 in GSE26253. All patients were divided into low and high groups by the median value of PRICKLE1. *P<0.05, **P<0.01, ***P<0.001. CCLE, Cancer Cell Line Encyclopedia. qRT-PCR, Quantitative real-time polymerase chain reaction.

metastasis mTOR signaling pathway. In our transcriptomic data, we also found that the genes involved in mTOR signaling were upregulated in metastatic LN compared with primary tumors (**Figure 6B**). Furthermore, phosphorylated mTOR and downstream phosphorylated

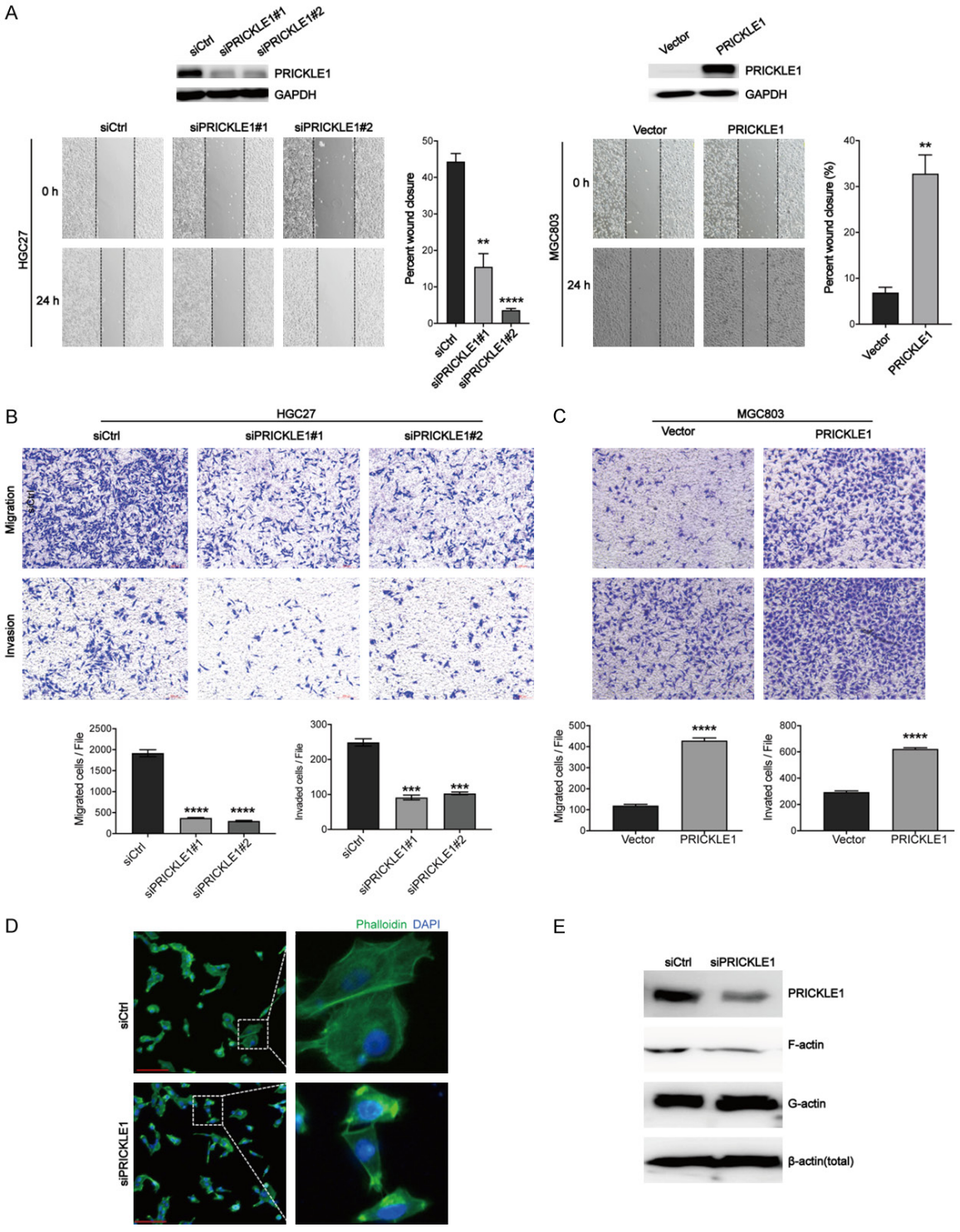

Figure 5. PRICKLE1 promoted GC migration and invasion in vitro. A: Wound healing assay of HGC27 transfected with siRNA targeting PRICKLE1 and MGC803 transfected with pCDNA3.1-PRICKLE1. B, C: Transwell assay of HGC27 transfected with siRNA targeting PRICKLE1 and MGC803 transfected with pCDNA3.1-PRICKLE1. D: Immunofluorescence of phalloidin staining was performed on HGC27 transfected with siRNA targeting PRICKLE1. Scale bar: 50 μm. E: HGC27 transfected with siRNA targeting PRICKLE1 was harvested. F-actin and G-actin were segmented by ultracentrifugation and analyzed by western blot. *P<0.05, **P<0.01, ***P<0.001, ****P<0.0001.

S6 ribosomal protein were inhibited when PRICKLE1 was downregulated in HGC27, while they were activated when PRICKLE1 was upregulated in MGC803 (**Figure 6C**). We further

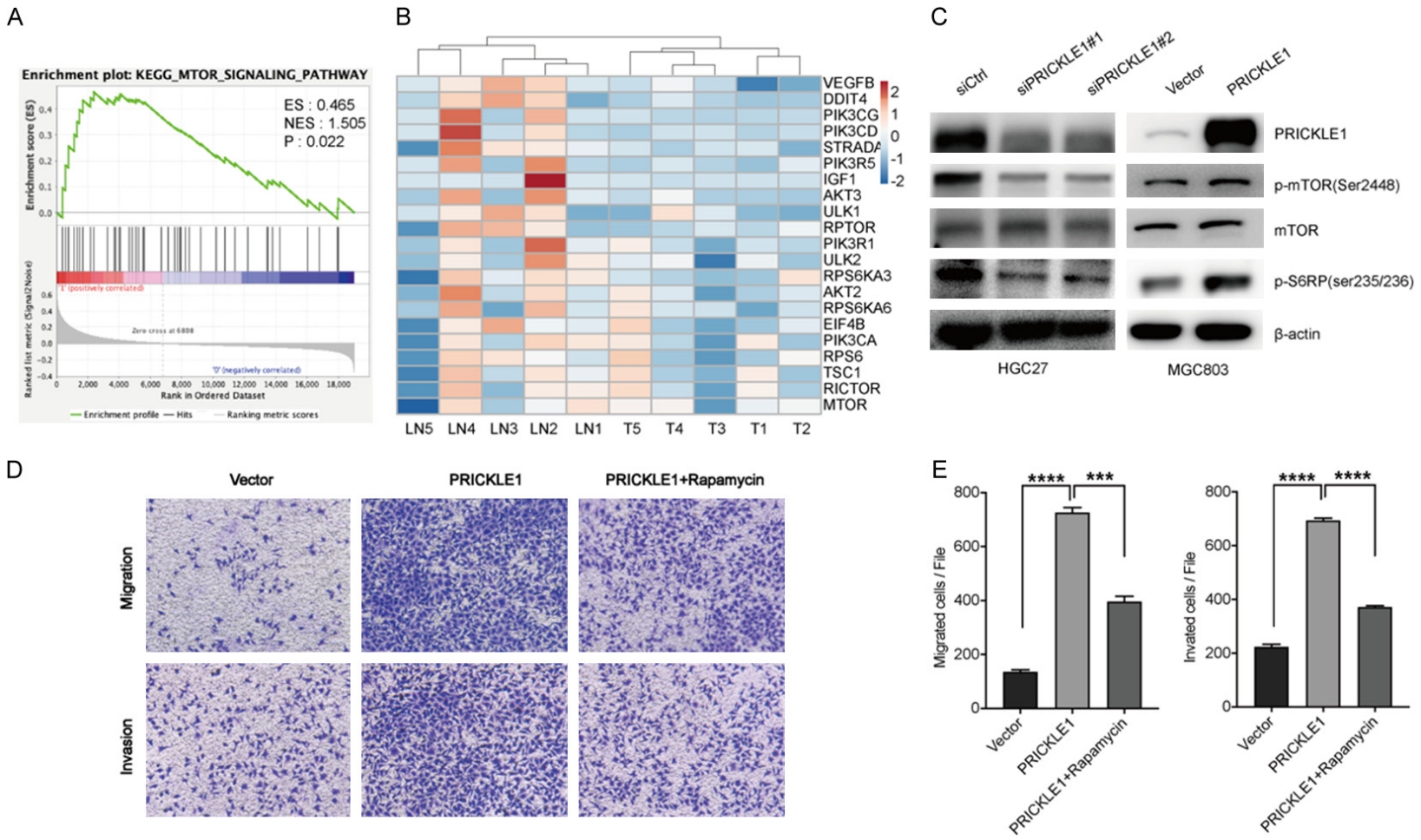

Figure 6. PRICKLE1 promoted GC migration and invasion by activating mTOR signaling. A: mTOR signaling activation was enriched in high PRICKLE1 patients by GSEA. B: RNA-seq data showed mTOR signaling was enriched in metastatic GC compared with primary GC. C: PRICKLE1 activated mTOR and downstream phosphorylated S6 ribosomal protein by western blot. D, E: The capability of migration and invasion of MGC803 transfected with pCDNA3.1-PRICKLE1 was reduced when mTOR inhibitor, Rapamycin, was applied. ***P<0.001, ****P<0.0001.

applied rapamycin, an inhibitor of mTOR signaling, in MGC803 with overexpressed PRICKLE1 and found that the migration and invasion capability was reduced (**Figure 6D**, **6E**). These data suggested that PRICKLE1 may promote GC metastasis by activating mTOR signaling pathway.

Discussion

Metastasis is the main cause of cancer-related death, including GC. Lymphatic metastasis has received much attention in recent years due to its strong indication of distant metastasis and shorter survival [17, 18]. But the driver genes and molecular mechanisms remain unclear in the process of lymphatic metastasis in GC. In the present study, we performed RNA-seq in metastatic GC from lymph nodes and paired primary tumor and identified several fundamentally upregulated genes in metastatic lymph nodes. Here, we focused on PRICKLE1, a protein regulating cell polarity and migration via modulating cytoskeleton. The previous study has reported its function in breast cancer metastasis [19], but its role in GC lymphatic metastasis remains to elucidate. We found that PRICKLE1 was highly expressed in metastatic GC cells and associated with the capability of migration and invasion. Mechanically, PRICKLE1 regulated migration and invasion by activating mTOR signaling. These results may provide a new insight to understand the mechanism of GC metastasis.

For identifying the driver gene involved in cancer metastasis, previous researches mainly focused on the differently expressed genes in the primary tumor and their relationship with the metastatic condition, like lymphatic metastasis, hepatic metastasis, and so on. Indeed, this relationship may not scientifically explain the mechanism of cancer metastasis, because these indicated genes may not be aberrantly expressed in metastatic lessons. Therefore, comparing the differently expressed genes in metastatic GC from lymph nodes could offer a chance to elucidate the mechanism of GC metastasis. In this study, we identified and validated several genes highly expressed in metastatic GC from lymph nodes. These genes have been previously reported to promote survival, proliferation, invasion, metastasis, and therapeutic resistance in several kinds of cancers. Consequently, our results indicated that these aberrantly expressed genes in metastatic GC may contribute to the process of metastasis and the mechanism is still needed to elucidate.

Here, we focused on PRICKLE1, which was an evolutionarily conserved protein and served as a member of the planar cell polarity pathway. This pathway is best known for its important role in epithelial tissue morphogenesis during embryonic development. Numerous studies have elucidated its fundamental role in cancer dissemination [20, 21]. Targeting the member molecules of this pathway has shown a therapeutic response for inhibiting breast cancer cell motility [22]. However, the function of PRICKLE1 in GC metastasis, especially lymphatic metastasis remains unknown. Our results showed that PRICKLE1 was dramatically overexpressed in metastatic GC and contributed to GC cell motility by the reorganization of the cytoskeleton. Accumulating evidence has indicated that cytoskeleton rearrangement and cell polarity modulation contributed to cancer motility and metastasis. Qiao and the team showed that Yes-associated protein (YAP) could promote GC metastasis by regulating the actin dynamic [16]. They found YAP modulated actin turnover and made cancer cells requiring a flexible cytoskeleton, which participated in cancer metastasis. However, how PRICKE1 affects the cytoskeleton remains unclear. Daulat and the team performed mass spectrometry analysis of the PRICKLE1 complex in the breast cancer cell and identified some interaction proteins associated with the cytoskeleton, like PHLDB2, CLASP1, ASPM [23]. These interactors combined with PRICKLE1 may contribute to cancer motility. In the present study, we showed high PRICKLE1 expression was correlated with mTOR signaling activation by GSEA. We further demonstrated that PRICKLE1 promoted mTOR phosphorylation and activated downstream phosphorylated S6 ribosomal protein. The migration and invasion capability were inhibited when mTOR inhibitor was applied. mTOR signaling acts as one of the critical downstream effectors of PI3K/AKT and contributes to metastasis and therapeutic resistance [24]. Daulat and the team discovered that activation of mTOR could enhance the migration capability and cancer cell dissemination via cytoskeleton reorganization [19]. In recent years, inhibi-

tion of mTOR activity has been reported to reduce metastasis and restore treatment response [25].

This study also contains certain limitations. First, we found PRICKLE1 as a novel regulator of GC metastasis. The detailed mechanism of lymph node metastasis from primary tumor involved a series of complex events, including changes in proliferation, metabolism, chemotaxis, lymphangiogenesis, and lymphatic drainage. More researches should be conducted to uncover the mechanisms of GC metastasis. Besides, although we found PRICKLE1 might promote GC cell migration and metastasis through cytoskeleton reorganization via the mTOR pathway, a more detailed regulatory mechanism remains to be elucidated in vivo and more clinical samples are needed to further illustrate and validate this finding.

In summary, we identified and validated a novel gene regulating migration and metastasis of GC via RNA-seq from clinical samples. PRICKLE1 may modulate GC cell migration and metastasis by actin cytoskeleton reorganization via the mTOR pathway. Our findings might provide valuable insight into the GC lymph node metastasis and the development of a potential therapeutic target to prevent GC dissemination.

Disclosure of conflict of interest

None.

Address correspondence to: Yihong Sun, Department of General Surgery, Zhongshan Hospital, Fudan University, 180 Fenglin Road, Shanghai 200032, China. Tel: +86-021-64041990; Fax: +86-021-64041990; E-mail: sun.yihong@zs-hospital.sh.cn

References

[1] Chen W, Zheng R, Baade PD, Zhang S, Zeng H, Bray F, Jemal A, Yu XQ and He J. Cancer statistics in China, 2015. CA Cancer J Clin 2016; 66: 115-132.

[2] Bray F, Ferlay J, Soerjomataram I, Siegel RL, Torre LA and Jemal A. Global cancer statistics 2018: GLOBOCAN estimates of incidence and mortality worldwide for 36 cancers in 185 countries. CA Cancer J Clin 2018; 68: 394-424.

[3] Van Cutsem E, Sagaert X, Topal B, Haustermans K and Prenen H. Gastric cancer. Lancet 2016; 388: 2654-2664.

[4] Karaman S and Detmar M. Mechanisms of lymphatic metastasis. J Clin Invest 2014; 124: 922-928.

[5] Roviello F, Rossi S, Marrelli D, Pedrazzani C, Corso G, Vindigni C, Morgagni P, Saragoni L, de Manzoni G and Tomezzoli A. Number of lymph node metastases and its prognostic significance in early gastric cancer: a multicenter Italian study. J Surg Oncol 2006; 94: 275-280; discussion 274.

[6] Lee HH, Yoo HM, Song KY, Jeon HM and Park CH. Risk of limited lymph node dissection in patients with clinically early gastric cancer: indications of extended lymph node dissection for early gastric cancer. Ann Surg Oncol 2013; 20: 3534-3540.

[7] Brown M, Assen FP, Leithner A, Abe J, Schachner H, Asfour G, Bago-Horvath Z, Stein JV, Uhrin P, Sixt M and Kerjaschki D. Lymph node blood vessels provide exit routes for metastatic tumor cell dissemination in mice. Science 2018; 359: 1408-1411.

[8] Pereira ER, Kedrin D, Seano G, Gautier O, Meijer EFJ, Jones D, Chin SM, Kitahara S, Bouta EM, Chang J, Beech E, Jeong HS, Carroll MC, Taghian AG and Padera TP. Lymph node metastases can invade local blood vessels, exit the node, and colonize distant organs in mice. Science 2018; 359: 1403-1407.

[9] Hood JL, San RS and Wickline SA. Exosomes released by melanoma cells prepare sentinel lymph nodes for tumor metastasis. Cancer Res 2011; 71: 3792-3801.

[10] Das S, Sarrou E, Podgrabinska S, Cassella M, Mungamuri SK, Feirt N, Gordon R, Nagi CS, Wang Y, Entenberg D, Condeelis J and Skobe M. Tumor cell entry into the lymph node is controlled by CCL1 chemokine expressed by lymph node lymphatic sinuses. J Exp Med 2013; 210: 1509-1528.

[11] Ubellacker JM, Tasdogan A, Ramesh V, Shen B, Mitchell EC, Martin-Sandoval MS, Gu Z, McCormick ML, Durham AB, Spitz DR, Zhao Z, Mathews TP and Morrison SJ. Lymph protects metastasizing melanoma cells from ferroptosis. Nature 2020; 585: 113-118.

[12] Li C, Sun YD, Yu GY, Cui JR, Lou Z, Zhang H, Huang Y, Bai CG, Deng LL, Liu P, Zheng K, Wang YH, Wang QQ, Li QR, Wu QQ, Liu Q, Shyr Y, Li YX, Chen LN, Wu JR, Zhang W and Zeng R. Integrated omics of metastatic colorectal cancer. Cancer Cell 2020; 38: 734-747, e739.

[13] Konieczkowski DJ, Johannessen CM and Garraway LA. A convergence-based framework for cancer drug resistance. Cancer Cell 2018; 33: 801-815.

[14] Hu Z, Ding J, Ma Z, Sun R, Seoane JA, Scott Shaffer J, Suarez CJ, Berghoff AS, Cremolini C, Falcone A, Loupakis F, Birner P, Preusser M, Lenz HJ and Curtis C. Quantitative evidence for early metastatic seeding in colorectal cancer. Nat Genet 2019; 51: 1113-1122.

[15] Daulat AM, Bertucci F, Audebert S, Serge A, Finetti P, Josselin E, Castellano R, Birnbaum D, Angers S and Borg JP. PRICKLE1 contributes to cancer cell dissemination through its interaction with mTORC2. Developmental Cell 2016; 37: 311-325.

[16] Qiao YT, Chen JX, Lim YB, Finch-Edmondson ML, Seshachalam VP, Qin L, Jiang T, Low BC, Singh H, Lim CT and Sudol M. YAP regulates actin dynamics through ARHGAP29 and promotes metastasis. Cell Rep 2017; 19: 1495-1502.

[17] Naxerova K, Reiter JG, Brachtel E, Lennerz JK, van de Wetering M, Rowan A, Cai TX, Clevers H, Swanton C, Nowak MA, Elledge SJ and Jain RK. Origins of lymphatic and distant metastases in human colorectal cancer. Science 2017; 357: 55-60.

[18] Gundem G, Van Loo P, Kremeyer B, Alexandrov LB, Tubio JMC, Papaemmanuil E, Brewer DS, Kallio HML, Högnäs G, Annala M, Kivinummi K, Goody V, Latimer C, O'Meara S, Dawson KJ, Isaacs W, Emmert-Buck MR, Nykter M, Foster C, Kote-Jarai Z, Easton D, Whitaker HC; ICGC Prostate Group, Neal DE, Cooper CS, Eeles RA, Visakorpi T, Campbell PJ, McDermott U and Wedge DC, Bova GS. The evolutionary history of lethal metastatic prostate cancer. Nature 2015; 520: 353-357.

[19] Daulat AM, Bertucci F, Audebert S, Serge A, Finetti P, Josselin E, Castellano R, Birnbaum D, Angers S and Borg JP. PRICKLE1 contributes to cancer cell dissemination through its interaction with mTORC2. Dev Cell 2016; 37: 311-325.

[20] Belotti E, Polanowska J, Daulat AM, Audebert S, Thome V, Lissitzky JC, Lembo F, Blibek K, Omi S, Lenfant N, Gangar A, Montcouquiol M, Santoni MJ, Sebbagh M, Aurrand-Lions M, Angers S, Kodjabachian L, Reboul J and Borg JP. The human PDZome: a gateway to PSD95-Disc large-zonula occludens (PDZ)-mediated functions. Mol Cell Proteomics 2013; 12: 2587-2603.

[21] Ciruna B, Jenny A, Lee D, Mlodzik M and Schier AF. Planar cell polarity signalling couples cell division and morphogenesis during neurulation. Nature 2006; 439: 220-224.

[22] Anastas JN, Biechele TL, Robitaille M, Muster J, Allison KH, Angers S and Moon RT. A protein complex of SCRIB, NOS1AP and VANGL1 regulates cell polarity and migration, and is associated with breast cancer progression. Oncogene 2012; 31: 3696-3708.

[23] Daulat AM, Finetti P, Revinski D, Silveira Wagner M, Camoin L, Audebert S, Birnbaum D, Kodjabachian L, Borg JP and Bertucci F. ECT2 associated to PRICKLE1 are poor-prognosis markers in triple-negative breast cancer. Br J Cancer 2019; 120: 931-940.

[24] Liu R, Chen Y, Liu G, Li C, Song Y, Cao Z, Li W, Hu J, Lu C and Liu Y. PI3K/AKT pathway as a key link modulates the multidrug resistance of cancers. Cell Death Dis 2020; 11: 797.

[25] deGraffenried LA, Friedrichs WE, Russell DH, Donzis EJ, Middleton AK, Silva JM, Roth RA and Hidalgo M. Inhibition of mTOR activity restores tamoxifen response in breast cancer cells with aberrant Akt Activity. Clin Cancer Res 2004; 10: 8059-8067.

Supplementary Table 1. The primers of indicated genes used in this study

Gene symbol	Forward	Reverse
PIK3IP1	CCAGCCTTCACGACAGAAAT	GTAGCCCAGAGTTCCCAGGT
PRICKLE1	ACTGGGCGATTCTGCTTATG	ATCCCGAACACTTTGCTCTG
NTRK3	ACAAGCCCACCCACTACAAC	AACCACCAACAGGACACAGG
FBLN1	CGATGTGGATGGAGTCACCT	TCTCGTTGATGGAGCAGTTG
PTGER3	ATCTCAGTCCAGTGCCCAGT	TTTCTGCTTCTCCGTGTGTG
PGM5	TCCTTCGGACCATCTTTGAC	CCTCCTTTCATTGCTTCCAG
18S-RNA	AGTCCCTGCCCTTTGTACACA	CGATCCGAGGGCCTCACTA

Supplementary Table 2. The detailed information of top 50 upregulated genes in metastatic lymph nodes from GC

Gene ID	Gene symbol	log_2FoldChange	*P* value
ENSG00000181092	ADIPOQ	10.72532536	5.65E-13
ENSG00000184811	TUSC5	8.900422418	2.05E-09
ENSG00000064205	WISP2	8.183997812	4.46E-09
ENSG00000164128	NPY1R	8.132321986	6.10E-11
ENSG00000054803	CBLN4	7.726658196	5.32E-06
ENSG00000170486	KRT72	7.238219816	8.37E-08
ENSG00000171759	PAH	6.981934591	0.003116878
ENSG00000101938	CHRDL1	6.854781529	1.36E-10
ENSG00000186049	KRT73	6.67312499	2.72E-08
ENSG00000166856	GPR182	6.575560102	9.79E-05
ENSG00000133636	NTS	6.384835178	0.000123969
ENSG00000152578	GRIA4	6.362568765	8.95E-07
ENSG00000111339	ART4	6.351310669	7.67E-14
ENSG00000170323	FABP4	6.225652249	5.92E-07
ENSG00000181234	TMEM132C	6.158762772	2.40E-07
ENSG00000171864	PRND	6.151599349	0.000817175
ENSG00000160505	NLRP4	6.091221928	0.000313654
ENSG00000150275	PCDH15	6.064964577	3.40E-05
ENSG00000182566	CLEC4G	6.03000941	3.30E-05
ENSG00000171819	ANGPTL7	6.014127312	0.007346149
ENSG00000104938	CLEC4M	5.950317431	0.00047561
ENSG00000174697	LEP	5.925298153	3.67E-05
ENSG00000163792	TCF23	5.796891618	0.001525515
ENSG00000101489	CELF4	5.794913112	0.000646165
ENSG00000162753	SLC9C2	5.645353068	0.000125802
ENSG00000136011	STAB2	5.642481465	1.78E-06
ENSG00000164530	PI16	5.622516632	1.82E-08
ENSG00000163273	NPPC	5.531287561	5.83E-05
ENSG00000170054	SERPINA9	5.524875055	8.65E-05
ENSG00000166819	PLIN1	5.484676148	1.40E-07
ENSG00000162391	FAM151A	5.460803233	6.21E-06
ENSG00000135447	PPP1R1A	5.45207484	0.000150976
ENSG00000179256	SMC03	5.44002852	0.000192501
ENSG00000198062	POTEH	5.406969313	0.004146824
ENSG00000106809	OGN	5.38605204	0.000221784
ENSG00000179542	SLITRK4	5.367730681	0.000387403

ENSG00000213231	TCL1B	5.295021784	0.009014681
ENSG00000184144	CNTN2	5.289101676	0.001283664
ENSG00000100362	PVALB	5.260720641	0.014889379
ENSG00000206579	XKR4	5.254739702	1.33E-05
ENSG00000106483	SFRP4	5.177424648	3.43E-05
ENSG00000188822	CNR2	5.17129246	8.58E-07
ENSG00000073754	CD5L	5.164126844	0.000511002
ENSG00000185915	KLHL34	5.156993558	0.001308611
ENSG00000070601	FRMPD1	5.122382819	0.000213053
ENSG00000116981	NT5C1A	5.12138862	3.94E-05
ENSG00000075429	CACNG5	5.110465391	0.010253543
ENSG00000196240	OR2T2	5.093233617	0.022434487
ENSG00000140538	NTRK3	5.075649598	2.34E-05
ENSG00000065609	SNAP91	5.073189348	1.67E-05

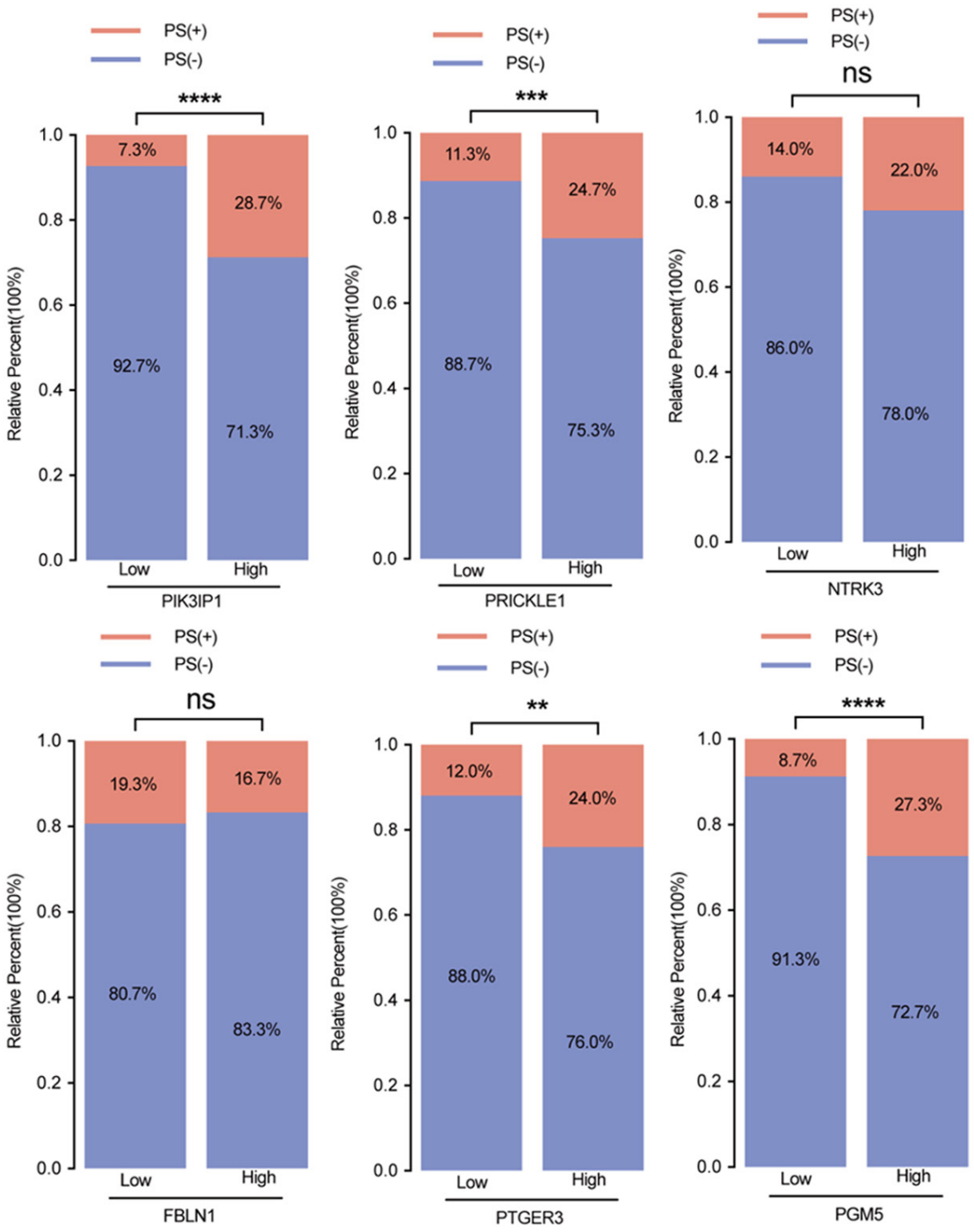

Supplementary Figure 1. The association between the expression of the six indicated genes and the peritoneal seeding (PS) status in GC.

Supplementary Table 3. the association between PRICKLE1 expression and the clinical pathological factors in ACRG cohort

Variable factors	PRICKLE1 expression		*P* value
	Low	High	
Age (years)			0.418
<65	77 (51.3%)	84 (56.0%)	
≥ 65	73 (48.7%)	66 (44.0%)	
Sex			0.020
Female	41 (27.3%)	60 (40.0%)	
Male	109 (72.7%)	90 (60.0%)	
Lauren classification			0.002
Intestinal	89 (59.3%)	61 (40.7%)	
Diffuse	56 (37.3%)	86 (57.3%)	
Mixed	5 (3.3%)	3 (2.0%)	
Perineural invasion			0.267
No	84 (67.7%)	75 (61.0%)	
Yes	40 (32.3%)	48 (39.0%)	
Venous invasion			0.049
No	72 (80.9%)	57 (67.9%)	
Yes	17 (19.1%)	27 (32.1%)	
Lymphovascular invasion			0.590
No	39 (27.7%)	34 (24.8%)	
Yes	102 (72.3%)	103 (75.2%)	
TNM stage			0.003
I/II	76 (50.7%)	51 (34.0%)	
III/IV	74 (49.3%)	99 (66.0%)	